Universal SSR Small Signal Stability Analysis Program of Power Systems and its Applications to IEEE Benchmark Systems

Dong-Joon Kim*, Hae-Kon Nam* and Young-Hwan Moon**

Abstract - The paper presents a novel approach of constructing the state matrix of the multi-machine power system for SSR (subsynchronous resonance) analysis using the linearized equations of individual devices including electrical transmission network dynamics. The machine models in the local d-q reference frame are integrated with the network models in the common R-I reference frame by simply transforming their output equations into the R-I frame where the transformed output is used as the input to the network dynamics or vice versa. The salient feature of the formulation is that it allows for modular construction of various component models without rearranging the overall state space formulation. This universal SSR small signal stability program provides a flexible tool for systematic analyses of SSR small-signal stability impacts of both conventional devices such as generation systems and novel devices such as power electronic apparatus and their controllers. The paper also presents its application results to IEEE benchmark models.

Keywords: SSR, network dynamics, eigenvalue analysis, small signal stability

1. Introduction

Based on the level of modeling details required, the small-signal oscillatory modes of a power system are divided into two categories: low frequency (LF) modes and high frequency (HF) modes. The stability of LF electromechanical oscillations in power systems involves the frequency range of 0.1 to 2.0 Hz. In this class of power system analysis, only the machine and its associated controllers are represented by nonlinear differential equations, but the dynamics of electrical transmission lines are neglected [1,2].

Depending upon the system parameters and the operating point, HF modes can become highly unstable. Torsional oscillations of turbine-generator (TG) sets [3,4], control interactions of fast acting devices, and interaction between TG torsional modes and controls [5] are examples of HF modes in the frequency range from 5 to 55 Hz. Eigenvalue analysis of HF modes requires the dynamic representation of the transmission network and its associated apparatus based on linearized differential equations [6].

Reference [6] reports a direct and useful approach for the formulation of state matrix from the linearized power system regarding an operating point including electrical transmission network dynamics, but its application to power systems is limited to the simple static var compensator (SVC), which is modeled in the common *R-I* reference frame. In addition, this method requires inefficient rotation of all machine models in the local *d-q* reference frame into the common *R-I* reference frame. References [7,8] take advantage of the time-domain simulation program to construct state-space equations by numerical differentiation. This method, however, is susceptible to inaccuracy due to numerical differentiation. Furthermore, it depends on the time-domain simulation program.

The method described in this paper uses a novel approach for constructing the state matrix of multi-machine power systems using the linearized equations of each device in its own frame. The complete set of the state matrix is derived, simply by transforming the output equations of both the machine and network into the other reference frame. The flexibility of modular construction [1,2,6,&7] adopted in the universal subsynchronous resonance (SSR) program allows for modeling a wide variety of power system components interconnected by an electrical transmission network, and makes the computer implementation of adding/modifying component models easier.

A wide range of the HF small signal stability problems in multi-machine power systems can be investigated with this proposed program: 1) SSR; 2) torsional oscillations as a result of interaction between a TG and either an HVDC converter, SVC or PSS; 3) control related problems and interaction among fast acting devices; and, 4) coordination of controllers. The proposed SSR analysis program has been tested against the IEEE First/Second benchmark models for SSR study [3].

* Dept. of Electrical Engineering, Chonnam National University, Korea. (djkim0419@keri.re.kr, hknam@chonnam.ac.kr)
** Electricity Market Technology Research Group, KERI, Korea. (yhmoon@keri.re.kr)
Received May 12, 2003; Accepted August 20, 2003

2. System Modeling

Two sets of state system matrices are derived separately: the linearized machine model is represented in the local *d-q* reference frame based on generator rotor with use of Park's transformation; the other is the set of the linearized state system matrix equations of an electrical transmission line in the common *R-I* reference frame. The overall system state matrix is then constructed by properly interfacing the machine and network state matrices. Model derivation of other devices, which are modeled in a common *R-I* reference frame like SVC, are not described in this paper, since it is the same as that of the transmission line.

2.1 Modeling Technique

In the process of formulating the machine equations, the generator terminal voltage in the local *d-q* reference frame is treated as the input, and the generator current is treated as the output. Incorporating the linear models of its associated apparatus such as the excitation system, PSS, and TG torsional system into the machine equations is straightforward. The overall linear model for the generating unit is represented as:

$$px_g = A_g x_g + B_g u_g + B_c v_c \tag{1}$$

$$i_{gg} = C_g x_g + D_g u_g + D_c v_c \tag{2}$$

where x_g is the state vector of the generator; u_g is the generator terminal voltage v_{gg}; i_{gg} is the generator terminal current; and v_c is the control inputs of the device. The matrices A_g through D_c are block diagonal. The symbol p means d/dt, and the symbol Δ for a small increment is omitted in this paper since it is clear that all linear equations are represented in terms of small perturbations.

For formulation of the network equations, all generators are replaced by independent current sources. The infinite bus is regarded as a generator bus, to which a HF classical machine with a large inertia is connected. The transmission lines are modeled with lumped *RLC* elements. This yields a linear *RLC* network with no dependent sources. For simplicity, the network reactance is considered to have no mutual inductance. The procedures for derivation of network state equations require a straightforward mathematical manipulation and are well described in [6,9]. The network equations are described by eqns. (3) and (4):

$$px_n = A_n x_n + B_n u_n + B_{1n} p u_n \tag{3}$$

$$v_{ng} = C_n x_n + D_n u_n + D_{1n} p u_n \tag{4}$$

where x_n is the network state vector; u_n is the set of generator current; and v_{ng} is the set of the generator voltage.

2.2 Interfacing Machine and Network

As described previously, the machine models are represented in a local *d-q* with coordinates based on the generator rotor. In contrast, the network equations are formed in a synchronously rotating *R-I* common reference frame. Note that each output and input of machine equations and network equations are reciprocals, i.e., each output of two systems is the input to the other systems. Therefore, it is necessary to transform each output in one frame into the other frame so that the other equations can make use of it as the input. The transformation matrices are as follows:

$$i_{gg} = i_{dq} = \begin{bmatrix} \sin\delta_0 & -\cos\delta_0 \\ \cos\delta_0 & \sin\delta_0 \end{bmatrix} i_{ng} + \begin{bmatrix} i_{r0}\cos\delta_0 + i_{i0}\sin\delta_0 \\ -i_{r0}\sin\delta_0 + i_{i0}\cos\delta_0 \end{bmatrix} \delta \tag{5}$$

$$v_{ng} = \begin{bmatrix} -V_0\sin\delta_0 & \cos\delta_0 \\ V_0\cos\delta_0 & \sin\delta_0 \end{bmatrix} v_{gg} \tag{6}$$

where $i_{gg}=[i_d,\ i_q]^T$, $i_{ng}=[i_R,\ i_I]^T$, $v_{ng}=[\theta_{RI},V_{RI}]^T$, and $v_{gg}=[\theta_{dq},V_{dq}]^T$. The generator terminal voltage is expressed in polar coordinates; phase and magnitude. By making use of the polar coordinates for the terminal voltages, it is possible to express the state equations of AVR in terms of the bus voltage and the solutions of load-flow calculations in the polar coordinate can then be directly utilized.

The overall state equations are obtained by transforming i_{gg} in eq. (2) and v_{ng} in eq. (4) to i_{ng} and v_{gg}, respectively, as in eqs. (5) & (6) and eliminating u_g, i_{gg}, u_n and v_{ng} in eqs. (1) & (3). Note that D_g and D_c in eq. (2) are zero. The overall system equations are given as:

$$p\begin{bmatrix} x_g \\ x_n \end{bmatrix} = \begin{bmatrix} N(A_g + B_g D_n' C_g') & NB_g C_n' \\ B_n C_g' + B_{1n} C_g' N(A_g + B_g D_n' C_g') & A_n + B_{1n} C_g' NB_g C_n' \end{bmatrix} \begin{bmatrix} x_g \\ x_n \end{bmatrix} + \begin{bmatrix} NB_c \\ B_{1n} C_g' NB_c \end{bmatrix} v_c \tag{7}$$

where $N=(I-B_g D_{1n}' C_g')^{-1}$ and C_g', C_n', C_{1n}' and D_n' are the transformed matrices using eqns. (5) and (6). These state equations have been implemented in the proposed HF dynamic stability program. This program can be used for SSR analysis, controller design, and frequency response calculations. The flexibility of the modular construction allows the easy addition and modification of a variety of excitation systems and prime mover models, HVDC links, loads and SVC.

3. Machine Modeling and Program Flow

Formulating the network state equations is fully described in [6] and therefore not reiterated here. The diverse simple machine models for SSR study have also been reported. However, for improved accuracy, it is necessary to obtain more sophisticated linear machine models based on the rigorous machine models such as those in PSS/E. In view of program efficiency, it is very important to use the rigorous machine models employed in transient stability study without modification. Note that in the HF stability study the dynamics of machine stators must be taken into account.

3.1 HF Machine Modeling

For improved efficiency and flexibility, it is necessary for the HF stability program to share the model data prepared for transient stability studies as much as possible. In other words, there is a definite benefit, in the HF stability program, to employ the linear models developed for the LF small-signal stability program as much as possible. The proposed HF stability program shares the nonlinear model data prepared for transient stability studies in PSS/E format. The only additional data needed for the HF program is mass and spring constants of the TG components. Furthermore, the models of various excitation systems and prime mover models for LF small-signal stability studies are used without modification. Thus, the efforts of preparing data and developing the linear model are reduced significantly.

Fig. 1-(a) shows general equivalent circuits for d-axis and q-axis flux linkage. Ideally, d-axis and q-axis flux linkage paths are de-coupled. However, more sophisticated generator models such as GENROU in PSS/E (shown in Fig. 1-(b)) include the effects of saturation and coupling between d-axis and q-axis. Though the dynamics of the stator windings are neglected in the LF stability studies, they must be considered in the HF stability. This necessitates the addition of two state equations including the speed voltage and rate of change of flux terms to system equations as follows:

$$p\psi_d = (v_d + r_a i_d + \omega_0 \psi_q + \psi_{q0}\omega)\omega_B \qquad (8)$$

$$p\psi_q = (v_q + r_a i_q - \omega_0 \psi_d - \psi_{d0}\omega)\omega_B \qquad (9)$$

where ω_B = 377.0 rad/s. These two linear equations represent the dynamics of the machine stator. In cases where the HF classical machine model is used for representing the infinite bus, only two linear equations associated with stator dynamics, eqs. (8) and (9), are considered.

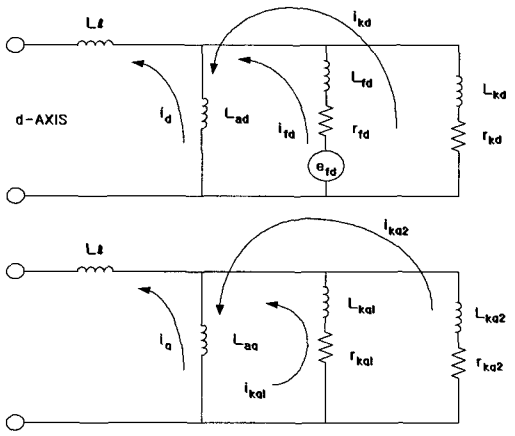

(a) Machine flux circuits

(b) Block diagram of round type machine model

Fig. 1 Block diagram of round type machine

3.2 Modeling of TG Torsional System

All TG torsional systems are comprised of multi-mass shaft systems. The proposed HF stability program is designed to accommodate up to 6-mass systems, as shown in Fig. 2. Single mass representation used in the LF stability study is also possible. The program can easily be modified to accommodate more than 6 mass systems if necessary.

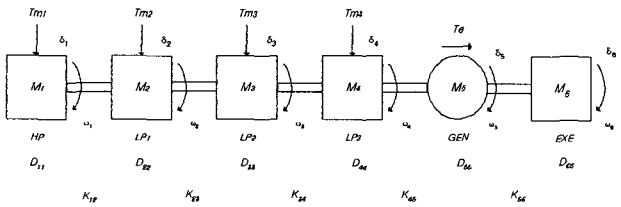

Fig. 2 Turbine-Generator 6-mass shaft system

3.3 Computation Procedures

Fig. 3 shows the computational flow in the proposed HF Stability Analysis program. The first step is to read the

load flow and run the load flow calculations. The typical load flow data includes bus data, generator data, transformer, and branch data. If a capacitor is installed, the corresponding data must also be provided.

After reading dynamic data, pre-calculations for the linearization of the nonlinear HF models (or LF models) are made at the "initializing" step using the results of load flow. The dynamic equations of network and machines are then formulated and interfaced. Finally, the eigenvalues, eigenvectors and partition factors are computed using the IMSL Math/Library [10] for analysis of HF small-signal stability.

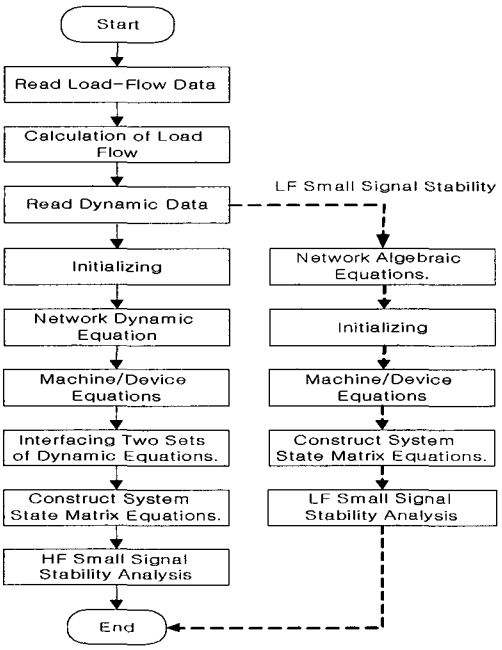

Fig. 3 Computational algorithm of HF eigenvalue program

In this program, the HF stability is of primary interest. However, the LF stability studies can be presented in a unified way using this program simply by removing the dynamics in the HF stability, which are not necessary in the LF stability. For example, the network dynamics and the multi-mass shaft system in the HF stability are represented by algebraic equations and the single mass lumped mass in the LF stability, respectively.

Currently, the order of the system matrix in which this software package can handle is about 500 at maximum because of the limitation in the IMSL. As more powerful software for eigenvalue analysis becomes available, the limitation on the size of the system matrix can be considerably eliminated.

4. Applications

The IEEE first/second benchmark models (FBM/SBM) for SSR study are used to test the integrity of the proposed HF stability program. The infinite bus is modeled with the HF classical machine model with a large inertia. In addition, the mechanical damping in the spring-mass system is ignored in these studies.

4.1 IEEE FBM for SSR Study

Fig. 4 shows the IEEE FBM for the computer simulation of SSR. This model has been widely used since 1977 for studying the torsional oscillations, evaluating the performances of study techniques and investigating SSR countermeasures. All the parameters are given in [3].

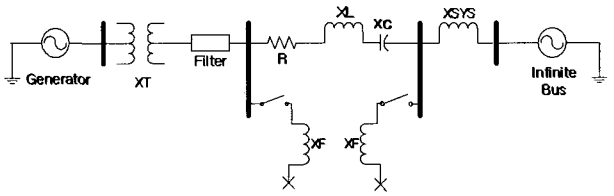

Fig. 4 IEEE FBM for SSR study (X_L=0.5 p.u.)

4.1.1 No-load Condition: P_e=0.0 p.u.

The computed eigenvalues of the IEEE FBM using the proposed HF stability program are shown in Table 1. It is found by observing the eigenvectors that the first four dominant modes with negative damping and mode 6 are associated with the TG modes. The fifth mode is a system mode associated with the oscillation of the entire rotor against the power system. The network modes (7 and 8) are associated with the *RLC* network. The rest of the modes, from 9 to 12 inclusive, are associated with the machine flux.

By comparing the real parts (decrement factors) of the four TG modes with those in reference [4], the accuracy of the proposed program is validated. They are almost identical, but there is a minor discrepancy in mode 1, which may have resulted from the differences in either the modeling or the eigenvalue computation routine used.

Table 1 The results of eigenvalues of IEEE FBM, V_t=1.0 p.u., Pe=0.0 p.u., *Xc*=0.371 p.u.

Mode No.	Real (1/s)	Imag. (rad/s)	Hz	Remarks
1	0.002 (0.028)	±202.860	32.286	TG /System Modes
2	0.025 (0.028)	±160.392	25.527	
3	0.103 (0.11)	±127.233	20.250	
4	0.048 (0.05)	±99.809	15.885	
5	-1.279	±10.805	1.720	
6	0.000	±298.176	47.456	
7	-4.374	±619.035	98.523	Stator/ Network Modes
8	-3.560	±134.303	21.375	
9	-25.414	0.0	0.0	Machine Modes
10	-23.002	0.0	0.0	
11	-1.266	0.0	0.0	
12	-0.948	0.0	0.0	

( ) *decrement factors Calculated from modal Mechanical Spring Mass Model [4]*

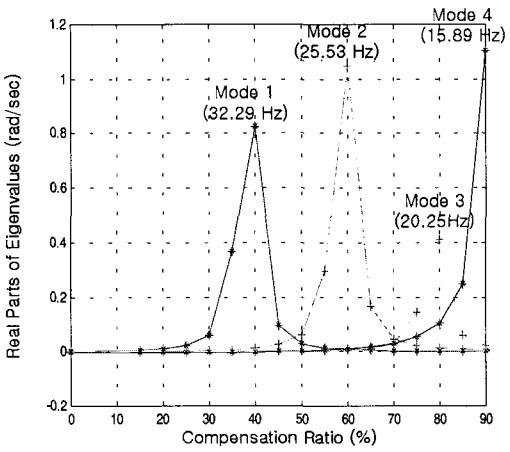

(a) The real parts of eigenvalues of TG modes versus X_C/X_L

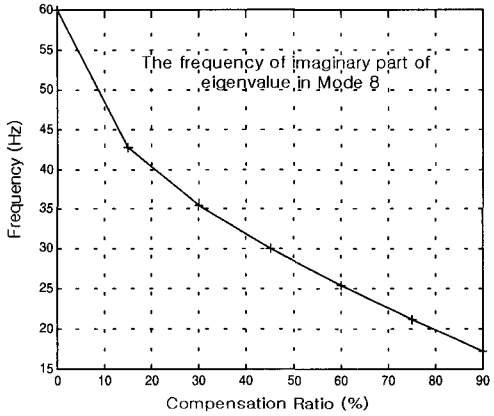

(b) The frequency of mode 8 (network mode) versus X_C/X_L

Fig. 5 The trajectory of the real parts of eigenvalues of the TG modes and the frequency of mode 8 versus X_C/X_L (no-load condition)

Figs. 5-(a) and 5-(b) show the trends of the real parts of the TG modes and the frequency of network mode 8 as the function of compensation ratio X_C/X_L, respectively. The peak in the negative damping of each TG mode occurs when the frequency of the network mode (mode 8) shown in Fig. 5-(b), passes the frequency of the corresponding TG mode. This suggests that the line compensation with X_C resulting in the frequency of the network mode near to that of any TG mode should be avoided. As shown in Fig. 5-(b), the frequency of mode 8 decreases gradually as the line compensation increases.

Fig. 6 shows migration of mode 5 (system mode) and mode 12 associated with the machine d-axis field time constant. The damping of the system mode is improved as the line compensation ratio increases. This observation is consistent with that in the LF stability, as low frequency oscillation problems are significant in the weak system where the machine is connected through the high external impedance. The machine mode is not affected significantly by the line compensation.

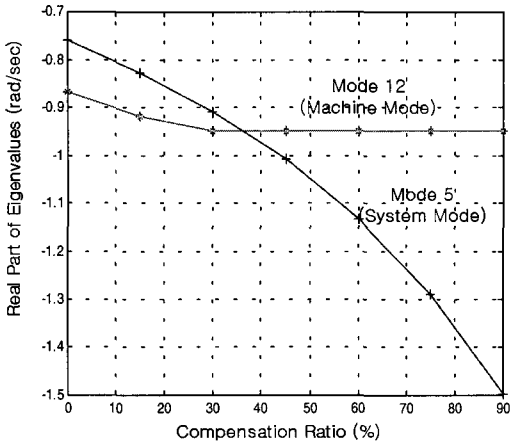

Fig. 6 The real parts of eigenvalues of mode 5 and mode 12 versus X_C/X_L (no-load condition)

4.1.2 Generator Loading: P_e=0.9 p.u.

Table 2 shows the eigenvalues computed at a higher generator loading. The loading condition is: P_e=0.9 p.u., 803.16MW, PF=0.9 lagging, terminal voltage, V_t=1.0 p.u., and X_C=0.371 p.u. The effects of the loading on the TG modes are different from mode to mode: mode 1 and 2 migrate into the stable region, but mode 3 and 4 become unstable. Mode 6 is unchanged. Notice also that mode 12, associated with rotor field flux, becomes unstable.

The trajectory of the real parts of the eigenvalues of the TG modes are plotted in Figs. 7 and 8 as a function of generator loading having a fixed 74% line compensation. Mode 4, which has the lowest natural frequency among the TG modes, is most vulnerable to an increase in the machine loading even though the frequency of mode 3, not mode 4, is closest to the network mode (mode 8) at 21 Hz. This suggests that an increase in generator loading may destabilize the TG modes as the line compensation increases.

Table 2 V_t=1.0 p.u., P_e=0.9 p.u., PF=0.9 lagging, X_C=.371 p.u..

Mode No.	Real (1/s)	Imag. (rad/s)	Hz	Remark
1	-0.030	±202.814	32.280	
2	-0.032	±160.314	25.525	
3	0.130	±127.103	20.238	TG/System
4	0.168	±99.426	15.841	Modes
5	-1.172	±9.187	1.462	
6	0.000	±298.177	47.456	
7	-4.365	±619.030	98.522	*Stator/ Net-*
8	-3.663	±134.450	21.398	work Modes
9	-25.424	0.0	0.0	
10	-23.069	0.0	0.0	Machine
11	-2.534	0.0	0.0	Modes
12	0.256	0.0	0.0	

* No mechanical damping represented in this study

Since mode 12 is a non-oscillatory mode and closely related to the voltage control loop, it may affect the synchronizing torque and lead to rotor angle instability. Actually,

time domain simulation using EMTDC [11] shows that when a three-phase fault is applied to the infinite bus for 0.12 seconds and then removed, loss of synchronism occurs shortly after the angle oscillation converges near to the steady state. In this case, the multi-mass system of the TG set is replaced by a single mass system in order to eliminate the effects of torsional interaction. By using the high-response excitation system [12], such an instability problem may be prevented.

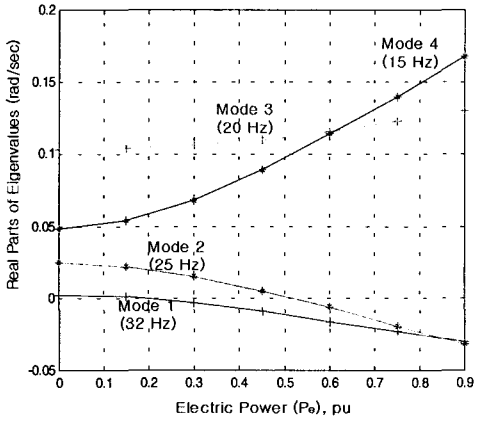

Fig. 7 The real parts of eigenvalue of TG modes versus increasing electric power, P_e(p.u.), Xc=0.371 p.u. (74% comp.)

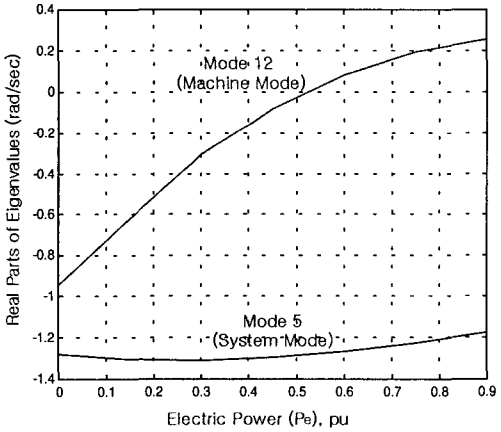

Fig. 8 The real parts of eigenvalue of Mode 5 and Mode 12 versus increasing electric power, P_e (p.u.), X_c=0.371 p.u. (74% comp.)

4.2 IEEE SBM System #1

Fig. 9 shows the IEEE SBM #1 where a single generator (600MVA) is connected to the infinite bus through two parallel lines, one of which is series compensated. This system is designed for study of negative damping due to self-excitation, which is calculated as a function of compensation. Compared with the FBM, the SBM System #1 is more practical with respect to the actual operation of a power system. All system parameters are given in [4].

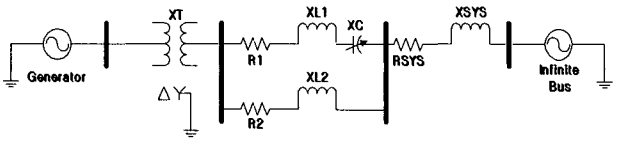

Fig. 9 IEEE SBM-System #1

4.2.1 No-load Case: P_e=0.0 p.u.

Table 3 shows the computed eigenvalues for the SBM System #1 with no-load and X_C=0.044 p.u. The first three modes (24 Hz, 32 Hz, and 51 Hz modes) are TG modes with negative dampings. Since the other modes are similar to those of the FBM, they are not described here in detail.

In order to validate the program, the real parts of modes 1 and 2 computed as a function of compensation in line #1 are listed in Table 4 and compared with those in [4]. In Table 4, "Proposed" and "IEEE" represent the real parts

Table 3 Eigenvalues of the SBM System # 1 with Xc= 0.044 p.u. (55%), V_t=1.0 p.u., P_e=0.0 p.u.

Mode No.	Real (1/s)	Imag. (rad/s)	Hz	Remarks
1	0.383	±155.239	24.707	TG/System Modes
2	0.005	±203.550	32.396	
3	0.001	±321.199	51.120	
4	-1.318	±9.632	1.533	
5	-15.620	±605.451	98.523	Stator/ Network Modes
6	-21.740	±376.862	60.000	
7	-15.382	±148.671	21.375	
8	-27.943	0.0	0.0	Machine Modes
9	-18.799	0.0	0.0	
10	-1.224	0.0	0.0	
11	-0.645	0.0	0.0	

* No mechanical damping represented in this study.

Table 4 Comparison of the real parts of modes 1 and 2 in the SBM System # 1, computed by the proposed program and reference [4]

Comp. (%)	Mode 1 (24 Hz)		Mode 2 (32 Hz)	
	Proposed	IEEE	Proposed	IEEE
0	-0.001	-	0.001	-
20	0.006	0.006	0.006	0.006
25	0.011	0.011	0.016	0.016
30	0.021	0.021	0.040	0.040
35	0.042	0.042	0.037	0.037
40	0.089	0.089	0.018	0.018
45	0.205	0.205	0.010	0.010
50	0.403	0.402	0.007	0.007
55	0.383	0.383	0.005	0.005
60	0.218	0.218	0.004	0.004
65	0.124	0.124	0.003	0.003
70	0.078	0.078	0.003	0.003
80	0.039	-	0.002	-
85	0.030	-	0.002	-
90	0.023	-	0.002	-

* No mechanical damping represented in this study.

computed by the proposed program and given in [4], respectively. The differences between the two results are negligible. The maximum negative damping occurs near the 50% compensation of the transmission line.

4.2.2 Generator Loading: P_e=0.9 p.u.

With the generator output of P_e=0.9 p.u., the eigenvalues of the SBM System #1 are shown in Table 5.

Table 5 Eigenvalues of the SBM System # 1 with Xc= 0.044p.u. (55%), V_t=1.0 p.u., P_e=0.90 p.u., PF=0.9 lagging

Mode No.	Real (1/s)	Imag. (rad/s)	Hz	Remarks
1	0.296	±154.993	24.668	
2	0.001	±203.527	32.392	TG /System
3	0.000	±321.197	51.120	Modes
4	-1.107	±7.773	1.237	
5	-15.618	±605.449	96.360	Stator/
6	-21.737	±376.866	59.980	Network
7	-15.299	±148.731	23.671	Modes
8	-27.790	0.0	0.0	
9	-19.143	0.0	0.0	Machine
10	-2.236	0.0	0.0	Modes
11	0.142	0.0	0.0	

* No mechanical damping represented in this study.

An increase in generator loading produces, to some extent, the same effect as an increase in the line compensation starting from the no-load condition: the negative damping in mode 1 is slightly reduced. Notice that mode 11 is unstable, which suggests that a non-oscillatory rotor angle instability may have been caused. The above observations are similar to those in the FBM case.

4.3 IEEE SBM System #2

The IEEE SBM System #2 shown in Fig. 10 consists of two generators (Gen. #1 = 600MVA, Gen. #2 = 700MVA), which are connected to an infinite bus through a single series compensated transmission line. This system is well suited for studying the parallel resonance and interactions between turbine-generators with a common mode.

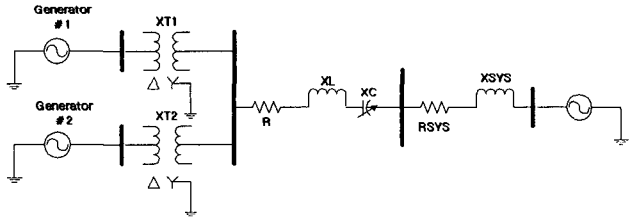

Fig. 10 IEEE SBM -System #2

4.3.1 No-load Condition: P_e=0.0 p.u.

The computed eigenvalues of this system with the no-load and X_C=0.0338 are listed in Table 6. There are 4 torsional modes with negative dampings. The frequencies of both mode 1 and mode 2 are approximately 24.8 Hz and very close each other. Mode 6 (1.826 Hz) and mode 7 (1.105 Hz) are the system modes with positive damping. Modes 8 and 10 are the network modes associated with *RLC* elements and mode 9 is the machine stator mode associated with the dynamics of the machine stators. The rest of the modes are associated with machine flux equations.

In Table 7, the real parts of modes 1 and 2 computed as a function of line compensation are compared with those in [4]. The differences between the two results are negligible. This proves again the validity of the proposed HF stability program.

Table 6 Eigenvalues of the SBM System # 2 with Xc= 0.0338 pu (65% Comp.), V_t=1.0, P_e=0.0

Mode No.	Real (1/s)	Imag. (rad/s)	Hz	Remarks
1	0.430	±155.785	24.794	
2	0.092	±155.641	24.771	
3	0.003	±203.559	32.397	TG/
4	0.000	±282.900	45.025	system
5	0.000	±321.200	51.121	Modes
6	-2.364	±11.473	1.826	
7	-0.894	±6.940	1.105	
8	-12.091	±586.347	93.320	Stator/
9	-6.319	±376.886	59.983	Network
10	-11.362	±167.019	26.582	Modes
11	-29.190	0.0	0.0	
12	-27.569	0.0	0.0	
13	-27.414	0.0	0.0	
14	-19.131	0.0	0.0	Machine
15	-1.710	0.0	0.0	Modes
16	-1.224	0.0	0.0	
17	-0.970	0.0	0.0	
18	-0.533	0.0	0.0	

* No mechanical damping represented in this study

Table 7 Comparison of the real parts of modes 1 and 2 in the SBM System # 2, computed by the proposed program and reference [4]

Comp. (%)	Mode 1 (24.79 Hz)		Mode 2 (24.77Hz)	
	Proposed	IEEE[4]	Proposed	IEEE[4]
0	0.003	-	-0.041	-
20	0.010	-	-0.039	-
40	0.031	-	-0.029	-
50	0.060	0.063	-0.006	-0.007
55	0.088	0.091	0.028	0.0259
60	0.127	0.133	0.114	0.1106
65	0.430	0.440	0.092	0.0863
70	0.938	0.951	0.022	0.0187
75	1.011	1.030	-0.005	-0.0073
80	0.607	0.622	-0.019	-0.0201
85	0.305	-	-0.026	-
90	0.166	0.1706	-0.031	-0.0316

* No mechanical damping represented in this study

4.3.2 Generator Loading: P_e=0.9 p.u.

With the generator output of P_{G1}=540MW and P_{G2}=

630MW, the computed eigenvalues of this system are listed in Table 8. All terminal voltages, including the infinite bus, are assumed to be 1.0 p.u.. The results are very similar to those of the no-load case except that damping and frequency of mode 7 (system mode) are significantly enhanced and reduced, respectively.

Table 8 Eigenvalues of the SBM System #2 with Xc= 0.0338 p.u. (65%), P_e=0.9 p.u., V_t=1.0

Mode No.	Real (1/s)	Imag. (rad/s)	Hz	Remarks
1	0.549	±155.646	24.294	TG /System Modes
2	0.155	±155.691	24.779	
3	-0.001	±203.533	32.393	
4	0.017	±281.459	44.796	
5	0.000	±321.198	51.120	
6	-1.450	±9.333	1.485	
7	-6.040	±1.399	0.223	
8	-12.119	±582.572	93.320	Stator/ Network Modes
9	-7.054	±376.465	60.394	
10	-11.201	±173.018	27.537	
11,12	-28.644	±0.098	0.016	Machine Modes
13	-26.825	0.0	0.0	
14	-19.816	0.0	0.0	
15	8.324	0.0	0.0	
16	-1.936	0.0	0.0	
17	-1.059	0.0	0.0	
18	0.131	0.0	0.0	

* No mechanical damping represented in this study

5. Conclusion

This paper described a novel yet efficient approach for the construction of the state matrix of multi-machine power systems for HF stability studies. By simply transforming the output equations of both machine and network state matrix equations into the other reference frame, a complete set of the state matrix equations is derived. The flexibility and modularity in constructing the state matrix allows for easy modeling of a wide variety of power system components, as well as the addition/modification of component models. The proposed HF stability program has also been tested and validated against the IEEE First/Second SSR benchmark models.

This universal SSR small signal stability program provides a flexible tool for systematic analyses of SSR small-signal stability impacts of both conventional devices such as generation systems and novel devices such as power electronic apparatus and their controllers.

Acknowledgements

This work was sponsored by the Advanced Power System Research Center at Korea University, and supported by the Ministry of Commerce, Industry and Energy in Korea.

References

[1] P. Kundur, G.J. Rogers, D.Y. Wang, and M.G. Lauby, M.G., "A comprehensive computer program package for small signal stability analysis of power systems', *IEEE Trans.*, PWRS-5, (4), pp. 1076-1086, 1990.

[2] Arabi, G.J. Rogers, D.Y. Wang, and P. Kundur, "Small signal stability program analysis of SVC and HVDC in power systems', *IEEE Trans., 1991, PWRS-6(3), pp. 1147-1153.*

[3] IEEE SSR Working Group, "First benchmark model for computer simulation of subsynchronous resonance", *IEEE Trans.*, Vol. PAS-96, September/October 1977.

[4] IEEE SSR Working Group, "Second benchmark model for computer simulation of subsynchronous resonance", *IEEE Trans.*, Vol. PAS-104, 1985.

[5] M. Bahrman, E.V. Larsen, R.W. Piwko, and H.S. Patel, "Experience with HVDC-Turbine-Generator Torsional Interaction at Square Butte", *IEEE Trans.*, 1980. PAS-99, (5), pp. 966-976.

[6] M. Parniani, M.R. Iravani, "Computer Analysis of Small-Signal Stability of Power Systems Including Network Dynamics", *IEE Proc-Gener. Transm. Distrib.* Vol. 142, No. 6, November *1995.*

[7] E.V. Larsen and W.W. Rice, "MANSTAB/POSSIM Power System Dynamic Analysis Programs - a New Approach Combining Nonlinear Simulation and Linearized State-Space/Frequency Domain Capabilities," *IEEE PICA Proceedings*, 1977, pp. 350-359.

[8] M.R. Iravani, "A Software Tool for Coordination of Controllers in Power Systems", *IEEE, Trans. On Power Systems*, Vol. 5, No-1, February 1990.

[9] E.S. Kuh and R.A. Rohrer, "The State Variable Approach to Network Analysis", *Proc., IEEE*, 1965, pp. 672-686.

[10] Visual Numerics, *IMSL Math/Library User's Manual Vol. 1*, 2000.

[11] Manitoba HVDC Research Centre, *PSCAD/EMTDC Power Systems Simulation Software Tutorial Manual*, 1994.

[12] F.P. DeMello and C. Concordia, "Concepts of Synchronous Machine Stability as Affected by Excitation Control", *IEEE Trans., Vol.* PAS-88, No. 4, pp. 316-329, Apr. 1969.

[13] P.M. Anderson, B.L. Agrawal, and J.E. Van Ness, *Subsynchronous Resonance in Power Systems, IEEE Press* 1990, pp. 233.

[14] P. Kundur, *Power System Stability and Control, McGraw-Hill, 1994.*

Dong-Joon Kim
He received B.S. and M.S. degrees in electrical engineering from Chonnam National University, Korea, in 1992 and 1994, respectively. He is now pursuing a Ph.D. degree from Chonnam National University. He has been with KERI since 1994 and is now a senior research engineer. His interests include analysis of voltage stability, dynamic modeling of power plants, control of HVDC modeling, and application of digital PSS. He is a Member of KIEE and IEEE.

Hae-Kon Nam
He received B.S. degree from Seoul National University, Korea, in 1975, M.S. degree from the University of Houston, Houston, Texas, in 1980, and Ph.D. degree from the University of Texas at Austin, Texas, in 1986, all in electrical engineering. From 1986 to 1988, he worked as a senior research engineer at KERI. Since 1988 he has been with Chonnam National University where he is now a Professor of Electrical Engineering. He was also a Visiting Professor at Pennsylvania State University and Powertech Labs Inc. in 1994 and 2001, respectively. His interests include power system stability and power plant modeling and control. He is a Member of KIEE and IEEE.

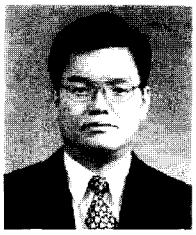

Young-Hwan Moon
He received B.S. and M.S. degrees from Seoul National University, Korea, in 1979 and 1981, respectively, and a Ph.D. from the University of Texas at Arlington in 1990, all in electrical engineering. He has been with KERI since 1981 and is now a principal research engineer. His interests include modeling of power systems, application of digital PSS, design of electricity markets and control of HVDC transmission. He is a member of KIEE, IEEE and Tau Beta Pi.